

Original Article

Fatigue performance and relaxation behavior of deep rolled martensitic stainless steel AISI 420

Laksamee Angkurarach and Patiphan Juijerm*

*Department of Materials Engineering, Faculty of Engineering,
Kasetsart University, Chatuchak, Bangkok, 10900 Thailand*

Received: 20 March 2019; Accepted: 15 October 2019

Abstract

Martensitic stainless steel AISI 420 was mechanically surface treated (deep rolled). Fatigue performance was evaluated using S/N curves. Residual stress and work hardening state relaxations during annealing and cyclic loading were investigated. Annealing processes were performed at temperature range of 300–600 °C and soaking time between 0.1–10⁴ min. Rotary bending fatigue tests were performed at stress amplitudes of 517–600 MPa with different number of cycles. The results of this study showed that residual stresses and work hardening states were thermally relaxed during annealing processes because of recovery and recrystallization mechanisms. Zener-Wert-Avrami function was used to analyze activation enthalpies of relaxation mechanisms. During cyclic loading, residual stresses were mechanically relaxed higher than that of the work hardening states.

Keywords: deep rolling, residual stress, relaxation, stainless steel, fatigue

1. Introduction

Martensitic stainless steels are widely used in many industries involving high static or cyclic loading with or without corrosive environment, such as structure parts, automotive parts, industrial tooling, cutlery, and mold (Chandler, 1995). Therefore, fatigue failure is a concerning aspect and higher fatigue lifetimes, as well as performances, are always expectations from end users. Mechanical surface treatments, i.e., deep rolling or shot peening provide near-surface compressive residual stresses and work hardening states inhibiting and retarding surface crack initiation and propagation (Juijerm & Altenberger, 2007; Schulze, 2006). Accordingly, fatigue lifetime enhancement of the mechanically surface treated condition could be expected. However, generated compressive residual stresses and work hardening states could be relaxed as well as decreased significantly under mechanical loading and/or elevated temperature (Eigenmann, Schulze & Vöhringer, 1994; Holzapfel, Schulze, Vöhringer & Macherauch, 1998; John, Buchanan, Caton & Jha, 2010; Lee & Mall, 2004;

Prevéy, 2000; Nikitin & Besel, 2008; Schulze, Vöhringer & Macherauch, 1993; Torres & Voorwald, 2002). Generally, the relaxation of residual stresses is associated with dislocation alteration. The easier dislocation movement, the higher residual stresses relaxation. However, for the work hardening relaxation, dislocation annihilations are required (Schulze, 2006). These relaxations will deteriorate the fatigue lifetime of mechanically surface treated metallic materials. Therefore, the stabilities of compressive residual stresses and work hardening states at the surface and in near-surface regions are very crucial for the fatigue lifetime enhancement of the mechanically surface treated metallic materials.

In this research, the fatigue performance, thermal and mechanical residual stress relaxations of the deep rolled martensitic stainless steel AISI 420 were studied. The Zener-Wert-Avrami function was used to describe the thermal relaxation behavior, whereas the mechanical relaxation behavior was analyzed using a logarithmic creep law.

2. Experimental Procedures

The investigated martensitic stainless steel AISI 420 was delivered as hardened and tempered bars with a diameter of 12.7 mm. The chemical composition of this alloy is 0.3% C, 0.25% Si, 0.43% Mn, 0.018% P, 0.028% S, 0.32% Ni,

*Corresponding author

Email address: fengppj@ku.ac.th; juijerm@gmail.com

12.15% Cr and Fe balance (all values in wt.%). Cylindrical specimens with a diameter of 7 mm and a gauge length of 20 mm were prepared according to the ASTM E466-96 standard. Fatigue tests were performed using a rotary bending fatigue tester. The deep rolling process was performed using a single roller burnishing tool with a diameter of 40 mm. A rolling pressure was 0.75 kN with a speed of 85 rpm. For the thermal relaxation, the deep rolled specimens were heated in a salt bath furnace at a temperature of 300–600 °C and annealing time between 0.1–10⁴ min. Residual stresses and work hardening states were measured on the surface before and after annealing treatments at the same position. Work hardening states were determined by full width and half maximum (FWHM) values of the X-ray peaks. For mechanical relaxation, the specimens were cyclically deformed using a rotary bending fatigue testing machine at stress amplitudes of 517, 550 and 600 MPa at room temperature for 1–10⁷ cycles. Fatigue tests were interrupted to measure residual stress and FWHM values at sample surfaces applying different cycle numbers at given stress amplitudes. Residual stresses and work hardening states of all specimens were measured using XRD technique with the classical $\sin^2\Psi$ method with Cr-K α radiation at the {211}-planes and $\frac{1}{2}S_2 = 6.16 \times 10^{-6} \text{ mm}^2/\text{N}$ as an elastic constant. Work hardening was characterized by the FWHM values of the X-ray diffraction peaks. The residual stress and FWHM values depth profiles were obtained using an electropolishing technique. All residual stresses and FWHM values were measured in longitudinal direction of the specimens.

3. Results and Discussion

3.1 Characterization and fatigue performance

After deep rolling at room temperature, near-surface compressive residual stresses, as well as work hardening states (represented by FWHM values), were characterized using XRD. Depth profiles of near-surface compressive residual stresses and FWHM values of the deep rolled martensitic stainless steel AISI 420 were constructed as shown in Figure 1. Compressive residual stress and FWHM values at the surface were -653.58 MPa and 2.82°, respectively, and they

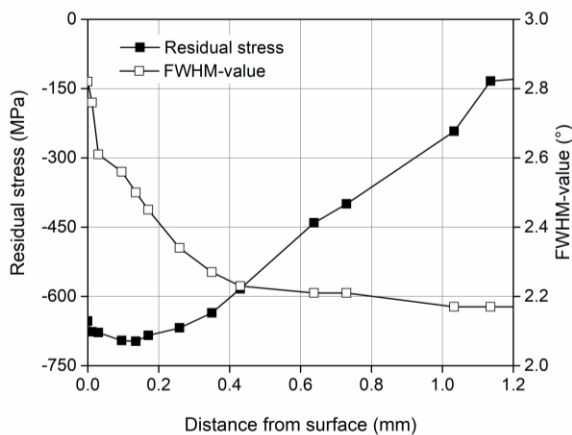


Figure 1. Depth profile of near-surface compressive residual stresses and FWHM values of the deep rolled martensitic stainless steel AISI 420.

continuously decreased with increasing distance from the surface. FWHM values of the substrate of approximately 2.2° were measured. It can clearly mention that the deep rolling induced near-surface compressive residual stresses and work hardening states. Moreover, it should be noted that higher near-surface FWHM values indirectly indicated the increased dislocation densities and stored strain energy at the surface and in near-surface regions (Lee & Mall, 2004). The near-surface compressive residual stresses and work hardening layer are benefits to enhance the fatigue lifetime of the deep rolled martensitic stainless steel AISI 420 because the crack initiation, as well as propagation, can be retarded (Jansawat, 2013; Nimitbunchar, 2014), especially at a high cycle fatigue regime. S/N curves of non- and deep rolled conditions were plotted and compared together in Figure 2. The deep rolling enhances fatigue lifetime of the martensitic stainless steel AISI 420, for example at a given stress amplitude of 500 MPa, the fatigue lifetime of the non-deep-rolled condition was about 133,000 cycles, whereas the deep rolled specimen was cyclically deformed till 10⁷ cycles without failure.

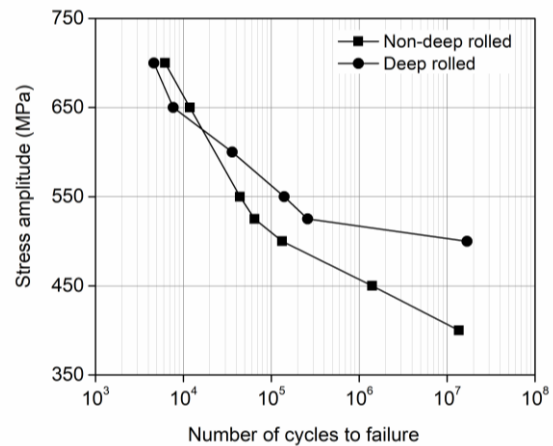


Figure 2. S/N curves of non- and deep rolled martensitic stainless steel AISI 420.

3.2 Effects of annealing on residual stresses and work hardening states

Compressive residual stresses and FWHM values at the surface of the deep rolled martensitic stainless steel AISI 420 were decreased with increasing annealing temperature and time as illustrated in Figure 3. This phenomenon can be attributed to thermally activated processes as recovery and recrystallization during annealing processes. At the temperature range of 300–500 °C (approximately lower than a half of the melting temperature), the relaxation was controlled by the recovery mechanism, whereas at a relatively high temperature of 600 °C, the recrystallization mechanism should take place during annealing. The thermally activated process is a major cause to decrease the stored strain energy resulting in dislocation movement, arrangement, and annihilation (Fu & Jiang, 2014; Zhan, Jiang & Ji, 2012). Furthermore, dislocation climb and slip during annealing are also a cause to decrease dislocation densities (Ren *et al.*, 2015; Xu *et al.*, 2017; Zhou *et al.*, 2012) of the deep rolled martensitic stainless steel AISI 420 at different annealing temperatures and time.

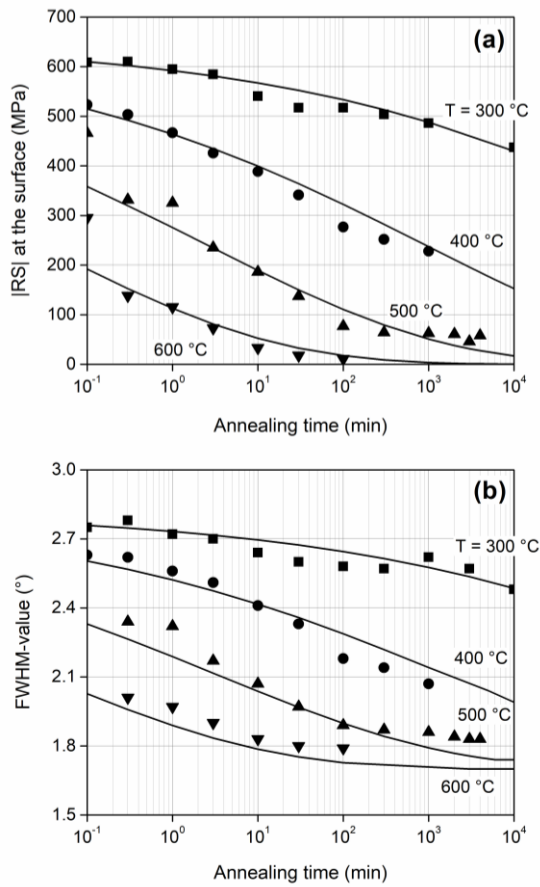


Figure 3. Absolute values of (a) residual stresses and (b) FWHM values at the surface of the deep rolled martensitic stainless steel AISI 420 at different annealing temperatures and time.

The relaxation of residual stresses and FWHM values are controlled by a thermally activated mechanism which can be described using the Zener-Wert-Avrami function as detailed in Equation 1 and 2 (Berger & Gregory, 1999; Chen, Liu, Wang, Xu, Ji & Jiang, 2018; Medvedeva, Bergstrom, Gunnarsson & Krakhmalev, 2011; Löhé & Vöhringer, 2002; Menig, Schulze & Vöhringer, 2003; Ren *et al.*, 2015; Telang, Gili, Mannava, Qian & Vasudevan, 2018; Wang, Chen & Jiang, 2011; Wang, Jiang & Ji, 2017; Xu *et al.*, 2017; Zhou *et al.*, 2012).

$$\sigma^{RS}/\sigma_0^{RS} = \exp[-(At_a)^m] \tag{1}$$

where σ_0^{RS} is the initial residual stress and σ^{RS} is the residual stress after annealing process at temperature T_a and time t_a , m is a numerical parameter dependent on the dominant relaxation mechanism, and A is a function dependent on the material and temperature according to:

$$A = B \exp(-\Delta H/kT_a) \tag{2}$$

where B is the material constant, k is the Boltzmann constant

($8.617 \times 10^{-5} \text{ eVK}^{-1}$), and ΔH is the activation enthalpy of the thermal relaxation process in the temperature and time range of this research. For the relaxation of FWHM values, the residual stress ratio, $\sigma_0^{RS}/\sigma_t^{RS}$ in the Zener-Wert-Avrami function has to be replaced by the ratio of $\Delta FWHM_{(T,t)}/FWHM_0$ from the experimental data. To obtain the parameter m , diagrams of $\log \ln (\sigma_0^{RS}/\sigma_t^{RS})$ and $\log \ln \Delta FWHM_0/\Delta FWHM_t$ as a function of $\log t_a$ at given annealing temperatures were depicted in Figure 4. Measured data were fitted by straight lines with a similar slope of approximately 0.16 for m_{RS} and m_{FWHM} . The activation enthalpy of the thermal relaxation was determined by the slope of the plot of $\log t_a$ and $1/kT_a$ in Figure 5. Activation enthalpies of thermal relaxation of residual stress and FWHM value relaxations were 2.64 and 2.77 eV, respectively. Other constants determined using experimental data were summarized in Table 1.

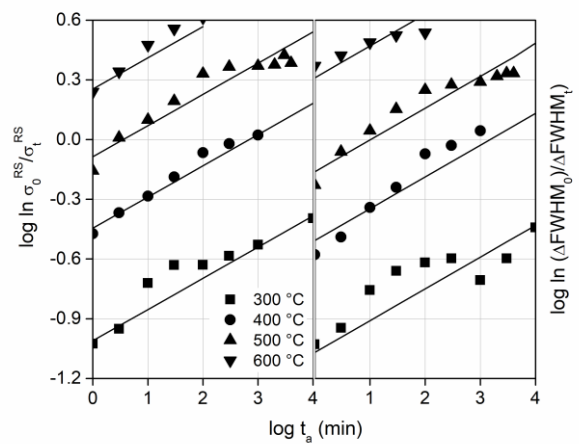


Figure 4. Plots of $\log \ln (\sigma_0^{RS}/\sigma_t^{RS})$ and $\log \ln (\Delta FWHM_0/\Delta FWHM_t)$ versus $\log t_a$ for the deep rolled martensitic stainless steel AISI 420 at different annealing temperatures.

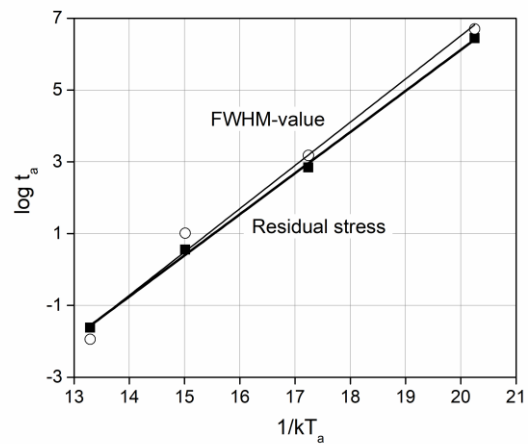


Figure 5. Plots of $\log t_a$ versus $1/kT_a$ for the determination of the Avrami approach parameters of the deep rolled martensitic stainless steel AISI 420.

Table 1. Determined materials constants of the thermal residual stress and FWHM-value relaxation of the deep rolled martensitic stainless steel AISI 420.

Deep rolled condition	m	ΔH (eV)	B (min^{-1})
Residual stress	0.16	2.64	6.10×10^{16}
FWHM-value	0.16	2.77	3.77×10^{17}

The experimental results showed that the activation enthalpy of FWHM value relaxation was slightly higher than that of thermal residual stress relaxation. The both activation enthalpies were close to the activation enthalpy of iron self-diffusion ($\Delta H_{\alpha\text{-Fe}} = 2.6 \text{ eV}$) [2,25]. Thus, it could be mentioned that the thermal relaxation of the deep rolled martensitic stainless steel AISI 420 was controlled by the volume diffusion-controlled climbing of edge dislocations (Eigenmann *et al.*, 1994; Fu & Jiang, 2014; Menig *et al.*, 2003; Prev y, 2000; Ren *et al.*, 2015). Thermally induced dislocation movements, as well as rearrangements as a recovery mechanism, caused the thermal residual stress relaxation, whereas the dislocation annihilations were additionally required for the thermal relaxation of the work hardening state (FWHM value) (Fu & Jiang, 2014; Schulze *et al.*, 1993). From Equation (1) and (2) combined with the determined parameters from experiments in Table 1, the residual stresses can be estimated at different annealing temperatures and times. Simulation diagrams of thermal residual stress relaxation of the deep rolled martensitic stainless steel AISI 420 were constructed for practical aspect as shown in Figure 6a and b. Additionally, the coefficient of correlation (R^2) and the mean absolute percentage error (MAPE) in Equation (3) were calculated showing accuracies as follows.

$$\text{MAPE} = \frac{1}{n} \sum_{i=1}^n \frac{E_i - P_i}{E_i} \times 100 \quad (3)$$

where E is the experimental data and P is the predicted data. The R^2 and MAPE of compressive residual stresses were about 0.97 and 15%, respectively. Demonstrating accuracy, all experimental data were compared to the predicted data in one diagram as shown in Figure 7.

3.3 Effects of cyclic loading on residual stresses and work hardening states

Compressive residual stresses at the surface of the deep rolled martensitic stainless steel AISI 420 decreased with increasing stress amplitudes and number of cycles as shown in Figure 8. The compressive residual stresses strongly decreased in the first cycle. Afterwards, compressive residual stresses decreased in a linear proportion to the logarithm of the number of cycles before fatigue failure occurred. From results in Figure 8, mechanical relaxations of compressive residual stresses were divided into three stages. Firstly, compressive residual stresses decreased considerably in the first cycle because of a quasi-static loading. The unstable dislocations created by deep rolling moved and rearranged immediately with the applied stress amplitude in the first cycle. Secondly, a linear dependence of compressive residual stresses with the logarithm of the number of cycles occurred according to a logarithmic creep law in Equation (4) (Boyce, Chen, Peters,

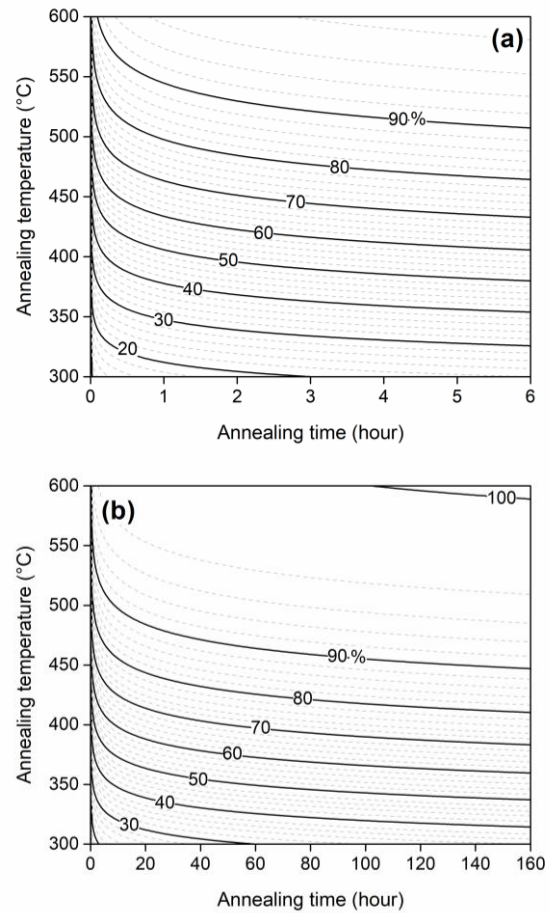


Figure 6. Simulation diagrams of residual stress relaxation in percent for (a) short and (b) extended periods using the Zener-Wert-Avrami function.

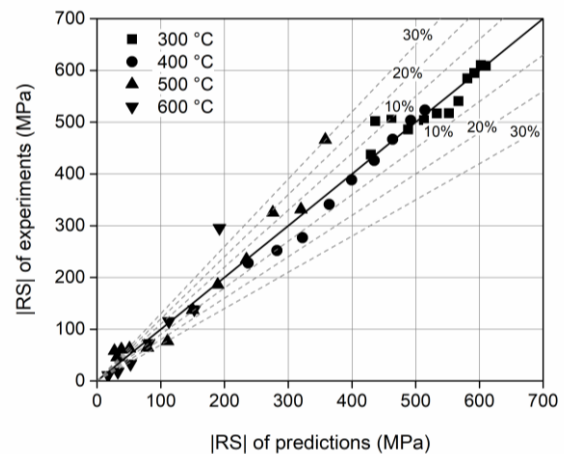


Figure 7. Comparison of experimental and predicted residual stresses in absolute values.

Hutchinson & Ritchie, 2003; Dalaei, Karlsson & Svensson, 2011; Juijerm, 2006; Kim, Cheong & Noguchi, 2013; Schulze, 2006; Zhuang & Halford, 2001).

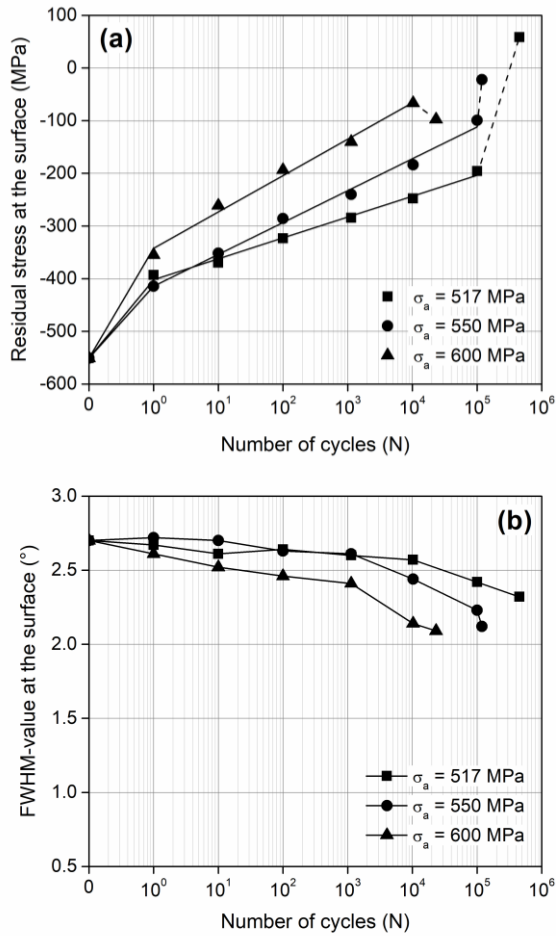


Figure 8. Mechanical relaxation of (a) residual stresses and (b) FWHM values at the surface of the deep rolled martensitic stainless steel AISI 420 at different applied stress amplitudes.

$$\sigma^{RS} = A(\sigma_a) - m(\sigma_a) \log N \quad (3)$$

where σ^{RS} is the residual stress after fatigue test at a given stress amplitude (σ_a) and number of cycle (N). Materials constants, A and m were determined by each stress amplitudes from experimental data in the linear sections of the curves and shown in Table 2. The materials constant m increased with increasing applied stress amplitudes, as a consequence of higher mechanical relaxation rate in the second stage (crack-free state) (Kim *et al.*, 2013). At higher stress amplitude, dislocations moved easier and then rearranged to lower energy structures. At the final state, the residual stress decreased unstably because of cracks or microcracks (Dalaei *et al.*, 2011; Kim *et al.*, 2013; Löhe & Vöhringer, 2002; Menig *et al.*, 2003).

The mechanical relaxation of FWHM values showed a different manner. The FWHM values at the surface were quite stable or slightly decreased with increasing number of cycles at the first and second states because dislocations moved, rearranged and partially annihilated. FWHM values decreased considerably after crack initiation at the third state

Table 2. Determined materials constants of the mechanical residual stress relaxation of the deep rolled martensitic stainless steel AISI 420.

Stress amplitudes (MPa)	Materials constant, m	Materials constant, A
517	39.62	-401.90
550	60.48	-414.34
600	69.15	-342.54

(Löhe & Vöhringer, 2002; Schulze, 2006). It can be mentioned that residual stresses were mechanically relaxed because of dislocation movements and rearrangements during cyclic loading, whereas the relaxation of the FWHM values required dislocation annihilations or microcracks.

4. Conclusions

The fatigue performance, thermal and mechanical relaxation behaviors of the deep rolled martensitic stainless steel AISI 420 were investigated and clarified. It can conclude as follows: (1) Near-surface compressive residual stresses and work hardening states induced by deep rolling enhanced the fatigue performance of the martensitic stainless steel AISI 420. (2) Thermal relaxations of residual stresses and work hardening states of the deep rolled martensitic stainless steel AISI 420 depended on annealing temperature and time taking into account the Zener-Wert-Avrami function. The activation enthalpies were 2.64 and 2.77 eV for residual stresses and work hardening states, respectively and comparable to the activation enthalpy of iron self-diffusion. (3) Compressive residual stresses were mechanically relaxed during cyclic deformation, especially in the first cycle. Afterwards, the logarithmic creep law can be used to describe before failure. The work hardening states were quite stable or slightly decreased with increasing number of cycles before failure.

Acknowledgements

Sincere thanks are expressed to the Faculty of Engineering, Kasetsart University, Thailand for financial support for L. Angkurarach. Thanks are due to the Iron and Steel Institute of Thailand (ISIT), Thailand for support of some experiments.

References

- Berger, M. C., & Gregory, J. K. (1999). Residual stress relaxation in shot peened Timetal 21s. *Materials Science and Engineering A*, 263(2), 200-204. doi: 10.1016/S0921-5093(98)01165-4
- Boyce, B. L., Chen, X., Peters, J. O., Hutchinson, J. W., & Ritchie, R. O. (2003). Mechanical relaxation of localized residual stresses associated with foreign object damage. *Materials Science and Engineering A*, 349(1), 48-58. doi:10.1016/S0921-5093(02)00543-9
- Chandler, H. (1995). *Heat treater's guide: Practices and procedures for irons and steels* (2nd ed.). Geauga, OH: ASM International.

- Chen, M., Liu, H., Wang, L., Xu, Z., Ji, V., & Jiang, C. H. (2018). Investigation on the thermostability of residual stress and microstructure in shot peened SAF 2507 duplex stainless steel. *Vacuum*, 153, 145-153. doi:10.1016/j.vacuum.2018.04.015
- Dalaei, K., Karlsson, B., & Svensson, L. E. (2011). Stability of shot peening induced residual stresses and their influence on fatigue lifetime. *Materials Science and Engineering A*, 528(3), 1008-1015. doi:10.1016/j.msea.2010.09.050
- Eigenmann, B., Schulze, V., & Vöhringer, O. (1994). Surface residual stress relaxation in steels by thermal or mechanical treatment. *Proceedings of the Fourth International Conference on Residual Stresses*. Baltimore, MD: Society for Experimental Mechanics Inc.
- Fu, P., & Jiang, C. (2014). Residual stress relaxation and micro-structural development of the surface layer of 18CrNiMo7-6 steel after shot peening during isothermal annealing. *Materials and Design*, 56, 1034-1038. doi:10.1016/j.matdes.2013.12.011
- Holzappel, H., Schulze, V., Vöhringer, O., & Macherauch, E. (1998). Residual stress relaxation in an AISI 4140 steel due to quasistatic and cyclic loading at higher temperatures. *Materials Science and Engineering A*, 248(1), 9-18. doi:10.1016/S0921-5093(98)00522-X
- Jansawat, P. (2013). *High temperature deep rolling on stainless steel AISI 420* [in Thai] (Master's thesis, Kasetsart University, Bangkok, Thailand).
- John, R., Buchanan, D. J., Caton, M. J., & Jha, S. K. (2010). Stability of shot peen residual stresses in IN100 subjected to creep and fatigue loading. *Procedia Engineering*, 2(1), 1887-1893. doi:10.1016/j.proeng.2010.03.203
- Juijerm, P. (2006). *Fatigue behavior and residual stress stability of deep-rolled aluminium alloys AA5083 and AA6110 at elevated temperature*. (Doctoral thesis, University of Kassel, Kassel, Germany).
- Juijerm, P., & Altenberger, I. (2007). Fatigue performance enhancement of steel using mechanical surface treatment. *Journal of Metals, Materials and Minerals*, 17(1), 59-65.
- Kim, J. C., Cheong, S. K., & Noguchi, H. (2013). Residual stress relaxation and low- and high-cycle fatigue behavior of shot-peened medium-carbon steel. *International Journal of Fatigue*, 56, 114-122. doi:10.1016/j.ijfatigue.2013.07.001
- Lee, H., & Mall, S. (2004). Stress relaxation behavior of shot-peened Ti-6Al-4V under fretting fatigue at elevated temperature. *Materials Science and Engineering A*, 366(2), 412-420. doi:10.1016/j.msea.2003.09.064
- Löhe, D., & Vöhringer, O. (2002). Stability of residual stresses. In G. Totten, M. Howes, & T. Inoue (Eds.). *Handbook of Residual Stress and Deformation of Steel* (pp. 54-69). Geauga, OH: ASM International.
- Medvedeva, A., Bergström, J., Gunnarsson, S., & Krakh malev, P. (2011). Thermally activated relaxation behaviour of shot-peened tool steels for cutting tool body applications. *Materials Science and Engineering A*, 528(3), 1773-1779. doi:10.1016/j.msea.2010.11.010
- Menig, R., Schulze, V., & Vöhringer O. (2002). Comparison of surface characteristics and thermal residual stress relaxation of laser peened and shot peened AISI 4140. *Proceedings of the 8th International Conference on Shot Peening*. Weinheim, Germany: Wiley-VCH.
- Nikitin, I., & Besel, M. (2008). Residual stress relaxation of deep-rolled austenitic steel. *Scripta Materialia*, 58(3), 239-242. doi:10.1016/j.scriptamat.2007.09.045
- Nimitbunchar, T. (2014). *Effects of heat treatment on residual stress and fatigue properties of deep rolled martensitic stainless steel AISI 420* [in Thai] (Master's thesis, Kasetsart University, Bangkok, Thailand).
- Prevéy, P. (2000). The effect of cold work on the thermal stability of residual compression in surface enhanced IN718. *Proceedings of the 20th ASM Materials Solutions Conference and Exposition*. Saint Louis, MO: ASM International.
- Ren, X. D., Zhou, W. F., Xu, S. D., Yuan, S. Q., Ren, N. F., Wang, Y., & Zhan, Q. B. (2015). Iron GH2036 alloy residual stress thermal relaxation behavior in laser shock processing. *Optics and Laser Technology*, 74, 29-35. doi:10.1016/j.optlastec.2015.05.009
- Schulze, V. (2006). *Modern mechanical surface treatment: States, stability, effects*. Weinheim, Germany: Wiley-VCH.
- Schulze, V., Vöhringer, O., & Macherauch, E. (1993). Thermal relaxation of shot peening induced residual stresses in a quenched and tempered steel 42CR Mo4. *Proceedings of the 5th International Conference on Shot Peening*. Coventry, England.
- Telang, A., Gill, A. S., Mannava, S. R., Qian, D., & Vasudevan, V. K. (2018). Effect of temperature on microstructure and residual stresses induced by surface treatments in Inconel 718 SPF. *Surface and Coatings Technology*, 344, 93-101. doi:10.1016/j.surfcoat.2018.02.094
- Torres, M. A. S., & Voorwald, H. J. C. (2002). An evaluation of shot peening, residual stress and stress relaxation on the fatigue life of AISI 4340 steel. *International Journal of Fatigue*, 24(8), 877-886. doi:10.1016/S0142-1123(01)00205-5
- Wang, C., Jiang, C., & Ji, V. (2017). Thermal stability of residual stresses and work hardening of shot peened tungsten cemented carbide. *Journal of Materials Processing Technology*, 240, 98-103. doi:10.1016/j.jmatprotec.2016.09.013
- Wang, Z., Chen, Y., & Jiang, C. (2011). Thermal relaxation behavior of residual stress in laser hardened 17-4PH steel after shot peening treatment. *Applied Surface Science*, 257(23), 9830-9835. doi:10.1016/j.apsusc.2011.06.032
- Xu, S. Q., Huang, S., Meng, X. K., Sheng, J., Zhang, H. F., & Zhou, J. Z. (2017). Thermal evolution of residual stress in IN718 alloy subjected to laser peening. *Optics and Laser Technology*, 94, 70-75. doi:10.1016/j.optlaseng.2017.03.004
- Zhan, K., Jiang, C. H., & Ji, V. (2012). Residual stress relaxation of shot peened deformation surface layer on S30432 austenite steel under applied loading. *Materials Transactions*, 53, 1578-1581.

- Zhou, Z., Bhamare, S., Ramakrishnan, G., Mannava, S. R., Langer, K., Wen, Y. H., . . . Vasudevan, V. K. (2012). Thermal relaxation of residual stress in laser shock peened Ti-6Al-4V alloy. *Surface and Coatings Technology*, 206(22), 4619-4627. doi:10.1016/j.surfcoat.2012.05.022
- Zhuang, W. Z., & Halford, G. R. (2001). Investigation of residual stress relaxation under cyclic load. *International Journal of Fatigue*, 23, 31-37. doi:10.1016/S0142-1123(01)00132-3